

Inertial Navigation Sensors

Neil M. Barbour

Charles Stark Draper Laboratory (P-5286)
Cambridge, MA 02139
USA

email: nbarbour@draper.com

ABSTRACT

For many navigation applications, improved accuracy/performance is not necessarily the most important issue, but meeting performance at reduced cost and size is. In particular, small navigation sensor size allows the introduction of guidance, navigation, and control into applications previously considered out of reach (e.g., artillery shells, personal navigation). Three major technologies have enabled advances in military and commercial capabilities: Ring Laser Gyros (RLGs), Fiber-Optic Gyros (FOGs), and Microelectromechanical Systems (MEMS) gyros and accelerometers. These technologies have generally replaced most mechanical gyros and many accelerometers in all but the higher accuracy applications. Mechanical sensors are a highly mature technology and are not discussed herein. RLGs and FOGs are now mature technologies also, although there are still technology advances underway for FOGs that may lead to miniature FOGs with relatively high performance. This is based on photonic crystal fibers that offer low loss and improved minimum bend radius limit. The Hemispherical Resonant Gyro (HRG) is also a mature technology with a niche in space applications and is briefly discussed. MEMS sensors are now widely available at the commercial level and starting to be available at the tactical performance level. These are based on numerous types of MEMS gyro designs using the Coriolis vibratory gyro principle. However, these have not yet matched the performance of tactical-grade RLGs and FOGs. Technology developments in the fields of optical gyros and MEMS gyros and accelerometers are described herein, based on ongoing advances in the inertial community. Emphasis is on MEMS sensor design and performance since it remains a very active development area. A relatively new technology based on cold atom interferometry is briefly discussed. Finally, predictions are made of how inertial sensor technology is expected to progress in the future.

1.0 INTRODUCTION

The science of guidance, navigation, and control (GN&C) has been under development for over 100 years. Many exciting developments have taken place in that time, especially in the area of navigation sensors [Refs. 1-18]. Today, to understand fully the entire range of navigation sensors, one needs to know a wide range of sciences, such as mechanical engineering, electronics, electro-optics, and atomic physics. Sensors are often compared on the basis of certain performance factors, such as bias and scale-factor stability and repeatability or noise (e.g., random walk). Sensor selection is made difficult by the fact that many different sensor technologies offer a range of advantages and disadvantages while offering similar performance. Nearly all new applications are strapdown (rather than gimballed) and this places significant performance demands upon the gyroscope (specifically: gyro scale-factor stability, maximum angular rate capability, minimum g-sensitivity, high bandwidth). For many applications though, improved accuracy/performance is not necessarily the driving issue, but meeting performance at reduced cost and size is. In particular, very small sensor size allows the introduction of GN&C into applications previously considered out of reach (e.g., artillery shells, 30-mm bullets), and many of these newer applications will require production in much larger quantities at much lower cost.

Inertial Navigation Sensors

The fact that an inertial (gyroscope or accelerometer) sensor's output drifts over time means that inertial navigation alone has an upper bound to mission accuracy. Therefore, various aiding/augmentation sensors have been tied into the inertial systems, e.g., Global Positioning System (GPS), velocity meters, seekers, star trackers, magnetometers, lidar, etc. The wide use of GPS aiding has allowed the use of much lower performing inertial sensors to achieve the required navigation solution. However, the fact that GPS may not always be available (e.g., from jamming or from being in an urban environment, indoors, or in tunnels and caves) or cannot be acquired quickly enough (such as very short-time-of-flight munitions) means that other navigation sensors will always be required. The key driver for which system architecture to use is cost for mission performance, where cost includes not only purchase but also life-cycle cost. Some mission applications have extreme size and power restrictions, so that not all inertial technologies are competitive.

Inertial sensors provide such a wide range of accuracy, that it has become useful to characterize them in terms of the application grade for which their accuracy is best suited. This is shown in Table 1. Clearly, there are other important performance parameters, such as noise (random walk) that would need to be considered for an actual application.

Table 1: Inertial Sensor Application Grades.

Application Grade	Gyro Performance	Accelerometer Performance
Consumer/Commercial	>1 deg/s	>50 mg
Tactical	~1 deg/h	~1 mg
Navigation	0.01 deg/h	25 μ g
Strategic	~0.001 deg/h	~1 μ g

In recent years, three major technologies in inertial sensing have enabled advances in military (and commercial) capabilities: the Ring Laser Gyro (since ~1975), Fiber Optic Gyros (since ~1985), and MEMS (since ~1995). RLGs enabled many new military missions because of their superior scale-factor stability and negligible g-sensitivity. FOGs have been developed as a lower cost alternative to RLGs and are employed in similar mission and system applications as RLGs. MEMS inertial sensors are a key enabling technology for miniature inertial navigation systems. The MEMS technology created a new marketplace for inertial navigation, namely guided tactical munitions and other emerging miniature GPS-integrated applications such as personal navigators. Figure 1 shows an overview of navigation technology insertion over the past century.

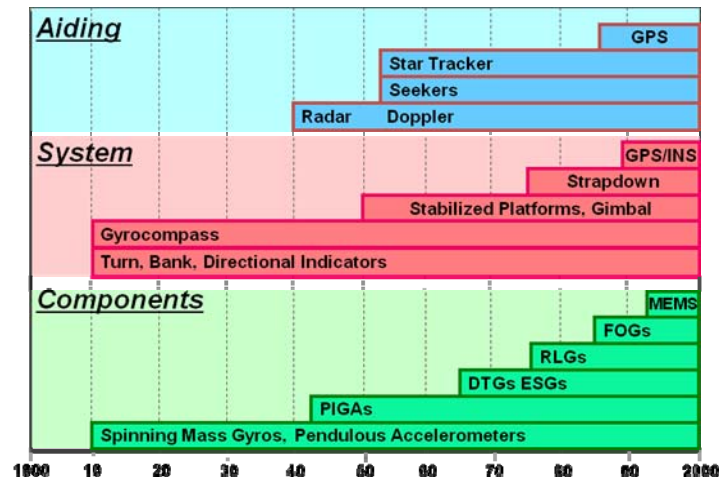


Figure 1: Technology Insertion History.

This paper discusses various ongoing gyroscope and accelerometer technology developments. Specific emphasis is given to the design and performance of MEMS sensors, which continues to be a very active development area.

2.0 INERTIAL SENSOR TECHNOLOGIES

The Ring Laser Gyro (RLG) moved into a market dominated by spinning mass gyros (such as rate gyros, single-degree-of-freedom (DOF) integrating gyros, and dynamically (or dry) tuned gyros) because it is ideal for strapdown navigation. The RLG was thus an enabling technology for high dynamic environmental military applications. FOGs were developed primarily as a lower cost alternative to RLGs, with expectations of leveraging technology advances from the telecommunications industry. FOGs are now matching RLGs in performance and cost, and are very competitive in many military and commercial applications. However, apart from the potential of reducing the cost, the FOG has not really enabled the emergence of any new military capabilities beyond those already serviced by RLGs. High-performance navigation-grade (0.01 deg/h and 25 μ g) RLG and FOG inertial measurement units (IMUs) are still expensive (>\$50 k) and relatively large (>100 cu in). Efforts to reduce size and cost resulted in the development of small-path-length RLGs and short-fiber-length FOGs. These did enable new military capabilities such as guided munitions (e.g., Joint Direct Attack Munition (JDAM)) and Unmanned Air Vehicles (UAVs) (e.g., Predator). However, as with all optical gyros, significant size reduction resulted in performance degradation even though cost reduction was achieved, so that these IMUs are around tactical-grade quality.

The potential for MEMS to provide low-cost, small-size navigation opportunities has resulted in an ongoing world-wide development effort geared toward consumer/commercial and tactical grade applications. The best currently available MEMS IMUs are around the 5 to 20 deg/h and 1 mg performance level, but have not yet reached true tactical-grade performance. MEMS IMUs and sensors are moving into the market currently dominated by tactical-grade FOGs and RLGs, as well as into new markets requiring small size and low cost.

2.1 Optical Gyros

2.1.1 Ring Laser Gyros (RLGs)

Although the **RLG** was first demonstrated in a square configuration in 1963, it wasn't until the late 1970s and 1980s that RLG systems came into common use as strapdown inertial navigators. The RLG is a laser that propagates light in clockwise (cw) and counterclockwise (ccw) directions simultaneously through a gas-filled optical cavity, using three or four mirrors. A schematic of a three-mirror RLG is shown in Figure 2. The RLG has excellent scale-factor stability and linearity, negligible sensitivity to acceleration, digital output, fast turn-on, excellent stability and repeatability across dormancy, and no moving parts. The RLG's performance is very repeatable under temperature variations so that a temperature compensation algorithm effectively eliminates temperature sensitivity errors. It is superior to spinning mass gyros in strapdown applications, and is an exceptional device for high dynamic environments. The RLG is an open-loop integrating gyro, i.e., its output is delta angle. However, taking samples over set time periods also provides angular rate information. Backscatter from the mirrors causes the two counterpropagating waves to lock frequencies at very low input rates, known as lock-in. This is overcome by introducing a frequency bias by means of a piezoelectric drive that dithers the RLG at several hundred hertz about its input axis. Lock-in has also been solved by incorporating a bent light path and a Faraday or Zeeman rotator to provide a four-beam multi-oscillator.

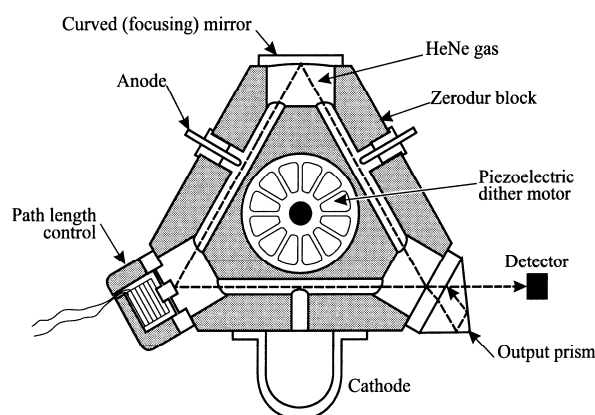


Figure 2: Ring Laser Gyro Schematic [Ref. 1].

RLGs and RLG systems are available from numerous manufacturers, such as Kearfott, Honeywell, Northrop Grumman, L-3 Communications, Thales (France), Sagem (France), iMAR (Germany), Astrophysika (Russia), etc. The Honeywell H-764G Embedded GPS/Inertial Navigation System (INS), which is based on GG1320 RLGs, is a 1-nmi/h navigator that has been installed on over 50 different aircraft types. Many ship navigation systems are now using laser gyro-based navigators (e.g., the Sperry Marine/Northrop Grumman MK 39 or the Honeywell MK 45). Northrop Grumman's ZLG™ (Zero-Lock™ Laser Gyro) is a four-mirror device that avoids lock-in by using a Faraday rotator and a bent light path to provide a four-beam multi-oscillator. The ZLG™ is thus two laser gyros in one, sharing identical optical paths, which reduces angle random walk (ARW) uncertainty. The ZLG™ is used in Northrop Grumman's LN100G navigation system. Navigation-quality laser gyro systems are on the order of 500 cu in (8,200 cc).

Efforts to reduce size and cost resulted in the development of small-path-length RLGs, such as Honeywell's 1308 and Kearfott's Monolithic RLG (MRLG), which are widely used in tactical-grade applications. As an example, the HG1700 IMU used in JDAM contains three 1308 RLGs. Kearfott's MRLG systems comprise

three RLGs in one block for size reduction; the T-10 three-axis RLG being approximately the size of a golf ball. Tactical-grade laser gyro IMUs are on the order of 40 cu in (650 cc).

The **RLG** is a mature technology, and current development efforts involve continued cost reduction rather than efforts at performance gains. There are some efforts to put RLGs on a chip, but performance is not expected to be any better than tactical grade. An example of miniaturization is the development of semiconductor ring lasers with a diameter of 3 mm. Thales (France) is also developing a miniature RLG. In general, small-size RLGs will continue to operate only in tactical-grade applications, so that eventually, MEMS IMUs will take over this market area.

2.1.2 Fiber-Optic Gyros (FOGs)

Development of the **FOG** began in the 1970s. The motivation was that the FOG was potentially less expensive and easier to build than the RLG and might be more accurate. In 1976, IFOG feasibility was demonstrated when an interference pattern (Sagnac effect) was discerned from light traveling cw and ccw around an optical fiber at the University of Utah. FOGs are sometimes referred to as Interferometric Fiber-Optic Gyros (IFOGs) because of their interference-based readout.

The **FOG** defines its light path by a wound coil of optical fibers in place of the RLG's mirrors and optical cavity (Figure 3). **FOGs** (also known as **IFOGs**) have an external broadband light source (e.g., superluminescent diode or doped fiber) that launches light into the fiber coil, which can be from 100 m to 3 km in length. Light from the optical source passes through a power splitter into an integrated optics circuit (IOC). The IOC splits the light into counterpropagating beams and then recombines them after they have traveled through the fiber coil. The recombined beam then retraces its path to the optical detector. The open-loop FOG is not an integrating gyro like the RLG, and the phase-angle output from the detector is proportional to angular rate. However, the FOG can be operated as an integrating gyro by the addition of a feedback loop from the detector to a frequency shifter in the integrated optics circuit. The feedback loop shifts the frequency of the light entering the coil so that the detector reads at null. The FOG is now operating closed-loop and the frequency shift measurement from the feedback loop is directly proportional to angle, provided feedback is at rates faster than the coil transit time.

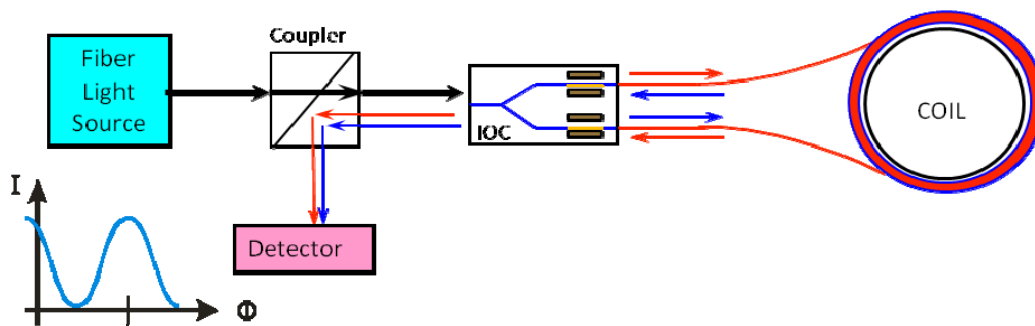


Figure 3: Open-Loop Interferometric FOG Schematic.

The FOG has some advantages over the RLG in that: the light source does not require high voltage; the broadband light source prevents backscatter so there is no lock-in at low input rates; and it has the potential for lower cost and lighter weight. A unique feature of the FOG is the ability to scale performance up and down. For example, doubling the coil length will decrease ARW by a factor of 2. However, unlike the RLG,

the open-loop IFOG is limited in dynamic range and only has moderate scale-factor stability. Thus, for most applications, closed-loop operation is preferred. One application where an open-loop FOG is being developed is for low-cost line-of-sight stabilization [Ref. 19].

The FOG has not yet superseded the RLG in production, due partly to the large existing RLG-based industrial infrastructure. However, FOGs continue to penetrate the market and have found applications in all performance areas, such as Unmanned Underwater Vehicles (UUVs) and UAVs, torpedoes, interceptors, camera and antenna stabilization, land navigation, Attitude and Heading Reference Systems (AHRS), gyrocompasses, and oil drilling. There are numerous manufacturers of FOGs and FOG IMUs such as KVH, Honeywell, Northrop Grumman (Litton), LITEF (Germany), Photonics (France), JAE (Japan), etc. In the tactical-grade area, Northrop Grumman's LN200 IMU may be the most widely known; many of which have silicon accelerometers. A space-qualified version, the LN200S, was used in the Mars Rover. To date, Northrop Grumman has built more than 50,000 tactical-grade fiber gyros. Northrop Grumman also has a navigation-grade FOG IMU, the LN250, for aircraft navigation. FOGs can also achieve extremely high performance [Refs. 20, 21], making them suitable for applications such as precise aiming of telescopes, imaging systems, and antennas, and for submarine navigation and strategic missile guidance. FOGs tend to have coils around 2 in (50 mm) diameter at the lower performance range and around 3 in (75 mm) or more in the higher performance range.

The **FOG** is a mature technology [Refs. 21-26] with performance and size comparable to the RLG. However, ongoing developments in solid-state optics and fiber technology could potentially lead to high performance in a miniature design. The development of photonic crystal fibers (PCFs) is underway for the communications industry and these offer advantages to the inertial sensor industry. In contrast to conventional optical fibers, PCF maintains superior mode confinement of the optical energy under sharp bend radius conditions, enabling the fabrication of small diameter (~2.5 cm) FOG sense coils. PCFs could also be used for further miniaturization to make optical ring resonators that are required for the development of a **Resonant FOG (RFOG)**. These technologies are described below.

2.1.3 Miniature FOGs

The development of **Miniature FOGs** (MFOGs) has taken advantage of recent ongoing technology developments in the communications field. One of them is PCF, which has the potential to be one of the enabling technologies for the next generation of FOG instruments. There are several key advantages of PCFs for FOG applications: (1) tight mode confinement results in bend losses much lower than conventional fiber. The limit on FOG coil diameter is primarily due to fiber winding losses and fiber size; (2) cladding diameters less than that for conventional fiber provide the potential for tighter fiber packing, resulting in smaller coils; (3) dispersion compensation can be incorporated into the PCF resulting in less spectral distortion; and (4) light guiding in an air-core photonic bandgap fiber offers the potential for utilizing mid-infrared optical wavelengths. Several vendors supply PCFs, such as NKT Photonics (Denmark), Corning, OFS, Blaze Photonics, etc. The lowest reported losses to date are 13 dB/km for air-core bandgap fiber at 1.5 μm (Corning) and 0.58 dB/km for silica index-guided holey fiber at 1.55 μm . Figure 4 shows examples of PCFs and the expected improvement of minimum bend radius. Figure 4 also shows the dimensions of an OFS fiber [Ref. 27] such that the diameter of the holes and the spatial period between the holes makes the fiber endlessly single mode, resulting in reduced relative intensity noise (RIN). Reference 27 also presents data from an open-loop PC-IFOG test bed at Draper Laboratory, with a sense coil length x diameter product of 2.9 in-km. The sense coil was constructed with solid-core PCF provided by OFS Laboratories. Earth's rotation was measured with an error less than 0.02 deg/h and ARW was 0.01 deg/ $\sqrt{\text{h}}$.

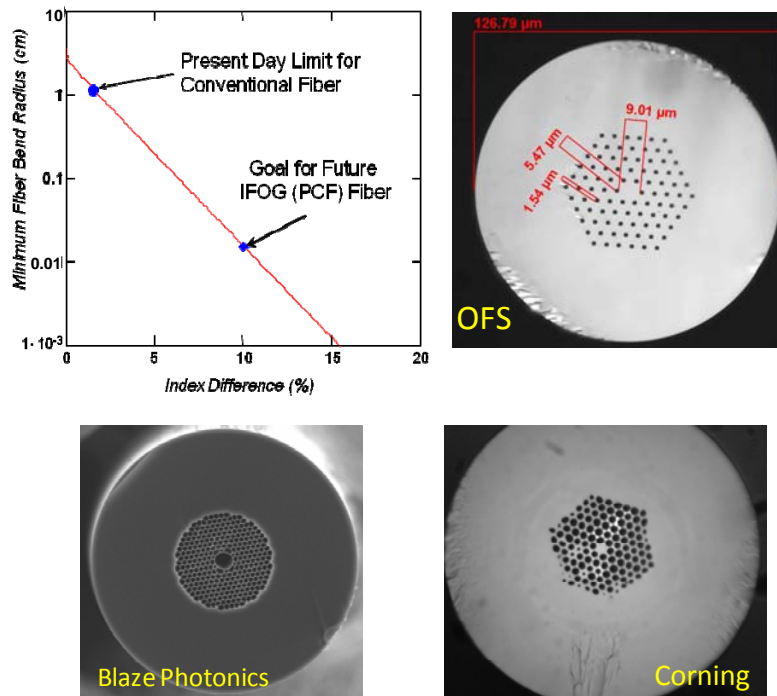


Figure 4: Photonic Crystal Fiber and Expected Improved Minimum Bend Radius Limit.

Another technology suitable for miniaturizing the FOG has been around since the early 1980s, but never perfected is the **RFOG**, which utilizes short lengths of fiber in which the cw and ccw light beams are kept in resonance. This requires a very narrow-band light source and low-loss fibers. RFOGs offer the potential for equivalent interferometric FOG performance, but with coil lengths up to 100 times shorter. Reference 28 presents a hollow core (photonic bandgap) fiber RFOG concept that may overcome the performance barriers of the past. Laboratory test data from a hollow core fiber ring resonator indicated very low losses and a stable resonance peak with low temperature sensitivity. Performance projections for an RFOG instrument using this fiber indicate that 0.001 deg/ \sqrt{h} ARW could be achieved with a 10-m fiber in a 10-mm diameter coil [Ref. 28].

Another step in miniaturizing FOGs is the development of a monolithic optical chip that contains the source and detector as well as the modulator. However, overcoming problems of backscatter and residual intensity modulation must be resolved. The combination of integrated optics and advanced fibers is one step toward reaching the ultimate in miniature optical gyros, the **Integrated Optics Gyro**.

2.1.4 Integrated Optics Gyroscope (IOG)

The RFOG architecture can be implemented in an **IOG** (or optical gyro on a chip), a tantalizing concept lurking around inertial sensor labs for several years. The IOG is an optical waveguide-based Sagnac effect gyroscope in which two beams of light travel in opposite directions around a waveguide ring resonator in place of an optical fiber. The relative position of the resonances is a measure of rotation rate about an axis that is perpendicular to the plane of the ring resonator. The IOGs are fabricated on wafers, combining the capabilities of integrated optic fabrication and MEMS fabrication. Figure 5 shows a schematic of an IOG with all of the components on-chip as well as a close-up of an optical waveguide.

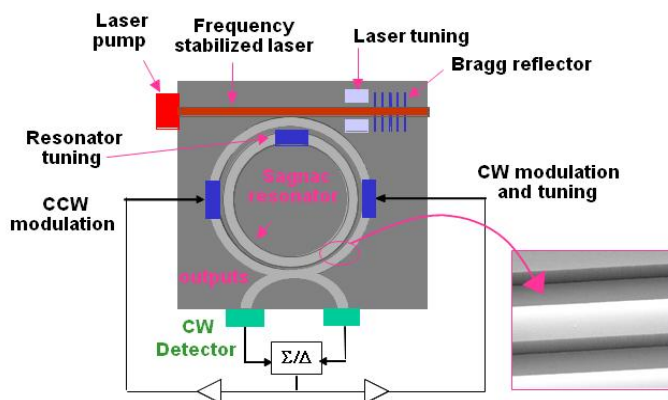


Figure 5: Integrated Optics Gyro (IOG).

One of the keys to achieving navigation-grade performance is to be able to manufacture waveguides with losses less than 0.001 dB/cm. Current state-of-the-art rare earth-doped waveguides have losses that are still one to two orders of magnitude away. Efforts are also ongoing to look at the advantages of slowing light to make an ultrasensitive optical gyroscope [Refs. 29, 30], but these are still at the basic research level.

A large part of the cost of current FOGs involves purchasing and connecting a variety of fiber pigtailed components. A planar lightwave circuit (PLC) can replace 21 components, significantly reducing cost. IOGs are expected to be in the size range of 0.2 cu in (3.25 cc) with power around 0.25 W. The IOG is targeted for applications currently met by RLGs, FOGs and MEMS. However, even commercial-grade IOGs are several years away.

2.2 Optical Accelerometers

Optical accelerometers are basically accelerometers that use an optical readout of the effect of acceleration on a physical structure. Although optical readouts have very high sensitivity, optical accelerometers have not found a niche since the performance is not readout limited. At present, none can be considered an enabling technology for military applications. Measurement of acceleration has been demonstrated using optical microspheres, in which the change in the light coupled into an optically resonant microsphere, as the sphere moves toward a waveguide, is detected. Incorporating optical readouts into MEMS devices has also been tried with varying success. Several efforts continue on the development of fiber-optic and fiber Bragg grating (FBG) accelerometers [Refs. 31, 32]. The advantages of an optical readout may only become apparent when resolving accelerations in the nano-g range for measuring seismic disturbances or gravity gradients. This means that the rest of the accelerometer's components must also be very low-noise. Reference 33 describes a novel accelerometer that monolithically integrates a Fabry-Perot interferometer and a photodiode. This is being marketed by Lumedyne Technologies.

The **Light Force Accelerometer (LFA)** is a novel device based upon the laser levitation of a dielectric particle proof mass. This basic idea was proposed over 30 years ago, but only recently has technology development driven by the telecommunications industry made a practical LFA possible. The LFA approach has several intrinsic advantages: it is a closed-loop approach, linear over many decades of inertial input; the approach is capable of extreme low noise and high sensitivity. A simplified LFA implementation is depicted in Figure 6. A particle is levitated against acceleration using a laser beam. A sensor (e.g., a split photodetector) is used to observe the particle position along the laser beam axis. As the acceleration along the

laser beam axis changes, the LFA varies the laser power difference to maintain the particle's axial position. The laser power is proportional to the acceleration applied to the particle. It has been estimated that with reasonable operating parameters, fundamental noise limits would permit an LFA subjected to a constant 1 g inertial input to achieve a 5 ng measurement error in only 10 s of averaging. This is at the performance level required for GPS-denied navigation, but is still at the laboratory demonstration stage.

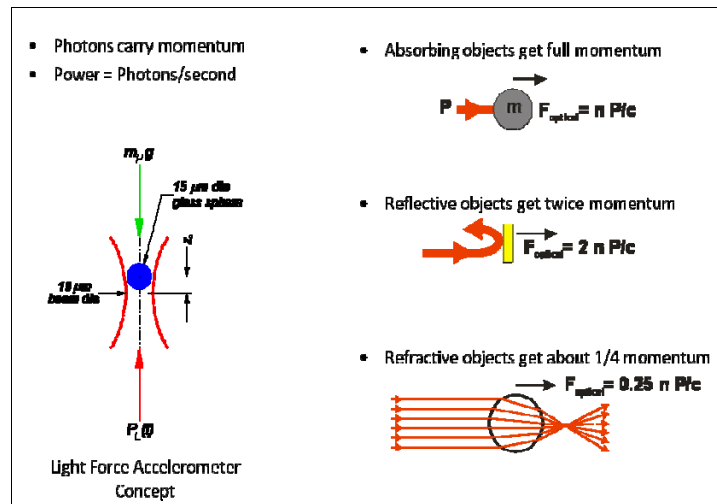


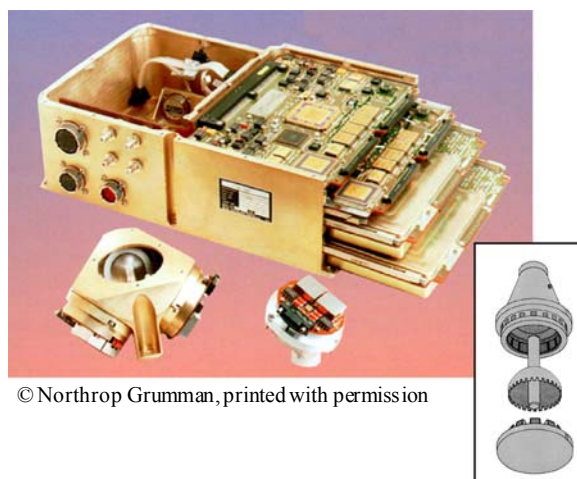
Figure 6: LFA Concept.

2.3 Hemispherical Resonant Gyro (HRG)

In the 1980s, Delco (now Northrop Grumman [Litton]) developed the **Hemispherical Resonator Gyro (HRG)**, which is a high-performance vibratory gyro whose inertially sensitive element is a fused silica hemispherical shell covered with a thin film of metallization. Electrostatic forcers surrounding the shell establish a standing resonant wave on the rim of the shell. As the gyro is rotated about its axis, the standing wave pattern does not rotate with the peripheral rotation of the shell but counter-rotates by a constant fraction (~0.3) of the input angle. Thus, the change in position of the standing wave, detected by capacitive pickoffs, is directly proportional to the angular movement of the resonator. In this mode of operation, termed whole angle mode, the HRG is an integrating sensor. The HRG can also be caged in a force rebalance mode to restrain the standing wave to a particular location and acts as a rate sensor. The whole angle mode is useful when excellent scale-factor stability and linearity are required over a wide dynamic range. The force-rebalance mode offers excellent angle resolution for pointing operations. HRG technology is also being developed in France and Russia.

The advantages of the HRG are that it is lightweight, very compact, operates in a vacuum, and has no moving parts, so that life expectancy is limited only by the electronics, which are provided redundantly for expected lifetimes of more than 15 years. It is a very high-Q device, so that vibrations of the shell persist for several minutes after power interruptions. This tends to make it immune to radiation and electromagnetic disturbances, since the pick-off can find the pattern mode and position when power is restored. It has negligible sensitivity to acceleration.

Since its debut in space in the mid-1990s, the HRG has been used on many spacecraft, including the Near Earth Asteroid Rendezvous (NEAR) spacecraft and the Cassini mission. Figure 7 shows a Space Inertial Reference Unit containing four HRGs whose hemispherical shells are 30 mm in diameter.



© Northrop Grumman, printed with permission

Figure 7: HRG Space Inertial Reference Unit.

2.4 MEMS Inertial Sensors

MEMS inertial sensors are expected to enable so many emerging military and commercial applications that they are becoming too numerous to list. MEMS is probably the most exciting new inertial sensor technology ever and development is a worldwide effort [Refs. 34-37]. Apart from size reduction, MEMS technology offers many benefits such as batch production and cost reduction, power (voltage) reduction, ruggedness, and design flexibility, within limits. However, the reduction in size of the sensing elements creates challenges for attaining good performance. In general, as size decreases, then sensitivity (scale factor) decreases, noise increases, and driving force decreases. Currently, the performance of MEMS IMUs continues to be limited by gyro performance [Ref. 38], which is now around 5-30 deg/h, rather than by accelerometer performance, which has demonstrated tens of μg or better.

There are now numerous suppliers of commercial-grade MEMS, many integrated with GPS. However, there are only a few suppliers of near-tactical-grade all-MEMS IMUs (Honeywell, Atlantic Inertial Systems (formerly BAE SYSTEMS), Northrop Grumman/LITEF). The appearance of a commercially-available MEMS system with performance of around 1 deg/h and hundreds of μg has been 'close' for the last few years, but has not yet materialized. When available, these will oust tactical RLG and IFOG systems in nearly all future applications.

2.4.1 MEMS Accelerometers

MEMS accelerometers detect acceleration in two primary ways: (1) the displacement of a hinged or flexure-supported proof mass under acceleration results in a change in a capacitive or piezoelectric readout; (2) the change in frequency of a vibrating element is caused by a change in the element's tension induced by a change of loading from a proof mass. The former includes the class usually known as pendulous or lateral displacement accelerometers and the latter are usually known as resonant accelerometers, or Vibrating Beam Accelerometers (VBAs). The pendulous types can meet a wide performance range from tactical systems to aircraft navigation-quality. VBAs, or resonant accelerometers, have the potential for even higher performance. Numerous types of MEMS accelerometers are being developed throughout the world at universities, government organizations, and in industry. Some examples of MEMS accelerometers are provided below.

2.4.1.1 Displacement-Based MEMS Accelerometers

Figure 8 shows a typical **out-of-plane (z-axis) MEMS displacement accelerometer**, in which a hinged pendulous proof mass, suspended by torsional spring flexures over a glass substrate, rotates under acceleration perpendicular to the plane of the device. Motion is detected via change in the capacitance gap using electrodes on an insulator substrate. Under a 1-g acceleration, the change in angle of the proof mass is typically around $70 \mu\text{rad}$; i.e., a $3 \times 10^{-8} \text{ m}$ change in sense gap, which results in a 12-fF (10^{-15}) peak change in capacitance. For a dynamic range of 15 g to $100 \mu\text{-g}$, it is necessary to resolve motion of $3 \times 10^{-12} \text{ m}$, or about 22.5 electrons charge change on the proof mass per carrier cycle.

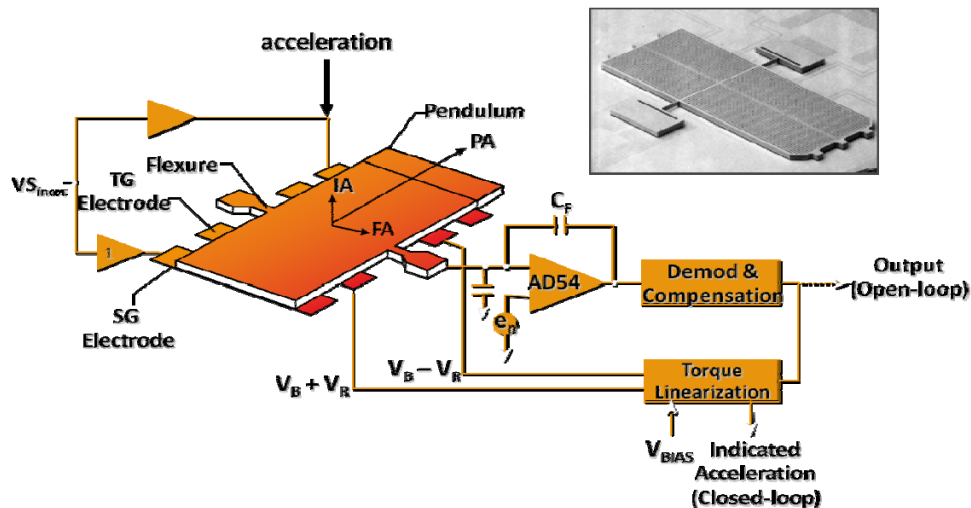


Figure 8: MEMS Pendulous Accelerometer.

A well-known example of this type of accelerometer is Northrop Grumman’s SiAc™, of which over 20,000 have been produced. Two versions have been developed (tactical grade and inertial grade) and have wide usage, such as AMRAAM, GMLRS, and Comanche helicopter. Other examples are Honeywell, Colibrys (Switzerland), Applied MEMS Inc., Silicon Designs, Sherborne Sensors (UK), Bosch (Germany), and numerous others.

Figure 9 shows a typical **in-plane (lateral) displacement accelerometer** in which proof mass displacement is measured by the change in capacitance across the comb fingers. This accelerometer is much more sensitive to accelerations in the left-to-right (rather than top-to-bottom) direction. The combination of z-axis and lateral accelerometers results in optimized system volume, since three axes of acceleration measurement can be achieved from three planar chips.

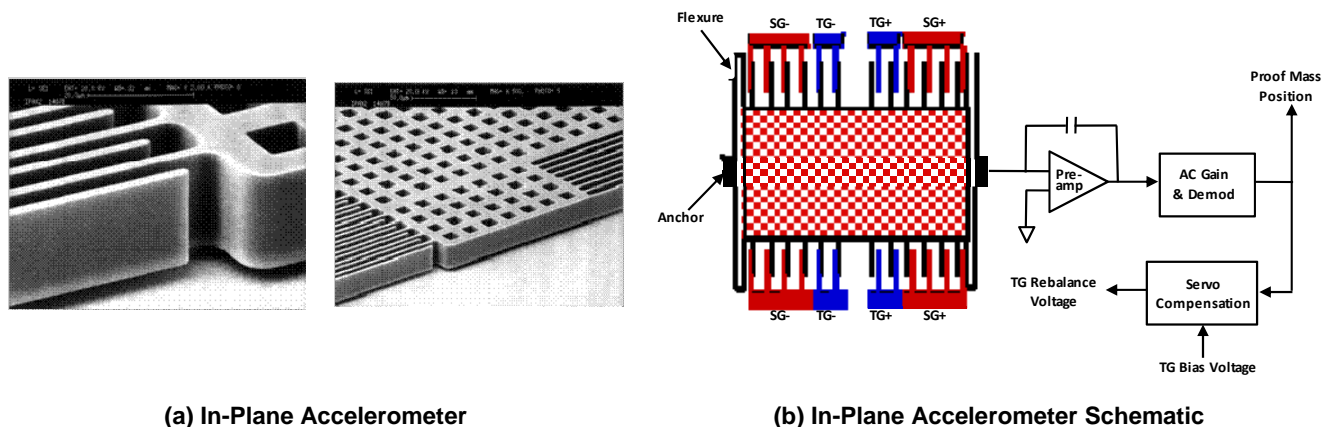
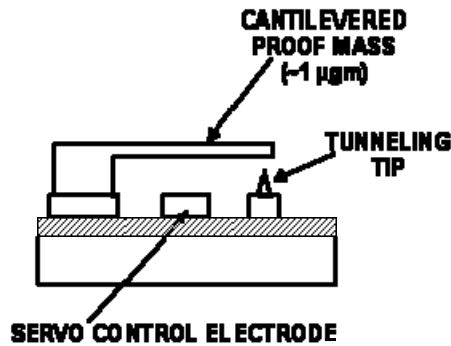


Figure 9: MEMS Lateral Accelerometer.

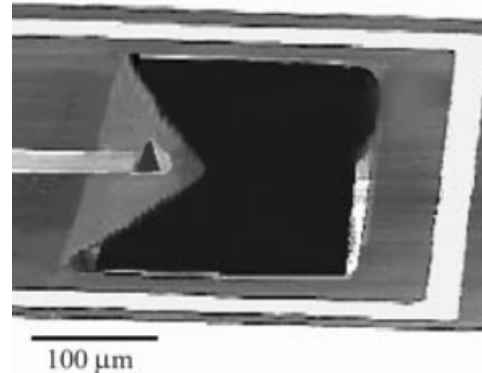
The most well-known of the commercial-grade in-plane accelerometers are probably the Analog Devices ADXL150 and ADXL250. The latter measures lateral accelerations in two axes with a noise floor of $1\text{mg}/\sqrt{\text{Hz}}$ and accuracy around 10-50 mg.

Displacement accelerometers can be operated open or closed loop. Colibrys [Ref. 39] has reported high accuracy for the RS9000 series accelerometers operating open loop in the out-of-plane and lateral configurations. Both devices are all-silicon construction, with the out-of-plane device having a cantilevered proof mass sandwiched between upper and lower electrodes. Performance quoted is $\sim 120\ \mu\text{g}$ in-run bias stability, 1-mg turn-on repeatability, 400-ppm scale-factor accuracy, and rectification of $65\ \mu\text{g}/\text{g}^2$. A temperature sensor and digital Application-Specific Integrated Circuit (ASIC) is integrated with the sensor package to furnish on-board 4th-order temperature compensation. Colibrys has also shown [Ref. 40] that a sigma-delta 5th-order regulation loop leads to a dramatic linearity improvement and consequently greatly reduced Vibration Rectification Error (VRE).

A technology under development (by Hughes Research Laboratory, Stanford University, and others) that offers a very high sensitivity readout for a z-axis displacement accelerometer is the tunneling accelerometer. Figure 10(a) shows a schematic of a tunneling accelerometer. The control electrode electrostatically deflects the cantilever into the tunneling position ($<1\ \mu\text{m}$ and $\sim 20\ \text{V}$). A servo mechanism holds constant the gap between the tunneling tip (Figure 10(b)) and the cantilever, and hence holds constant the tunneling current ($\sim 1\ \text{nA}$). The output signal is the change in voltage at the electrode under acceleration. These devices are designed to resolve accelerations in the nano-g range and require low-resonant frequency proof masses and sub-angstrom resolution readouts. Recent microfabricated tunneling accelerometers have resolved $20\ \text{ng}/\sqrt{\text{Hz}}$ over 5 Hz to 1.5 kHz [Ref. 41] with a closed-loop dynamic range of over 90 dB. However, maximum acceleration measurement capability is very low ($\sim 1\ \text{mg}$) without further loop modification. A tunneling accelerometer in China [Ref. 42] has exhibited good low frequency resolution of $15\ \text{ng}/\sqrt{\text{Hz}}$ over 1 to 100 Hz.



(a) Output is voltage required to keep cantilevered beam in fixed tunneling position during acceleration [Ref. 41]



(b) A scanning electron microscopic (SEM) view of triangular nitride cantilever and tunneling tip [Ref. 41]

Figure 10: MEMS Tunneling Accelerometer.

2.4.1.2 MEMS Resonant Accelerometers

Resonant accelerometers cover the general category of VBAs and can be z-axis or lateral. In resonant accelerometers, acceleration is sensed as a change in the resonant frequency of beam oscillators under the inertial loading of a proof mass, rather than measuring the mass displacement. The change in resonant frequency can be measured capacitively or piezoelectrically. In the latter, a piezoelectric resonator is micromachined (or deposited) in an area of high stress on one or more beams or flexures. As the flexure bends under proof mass motion, the resonant frequency changes accordingly. Examples of the piezoelectric type are: Systron Donner's Vibrating Quartz Accelerometer (VQA); Kearfott's Silicon Micromachined Vibrating Beam Accelerometer (MVBA); Honeywell's SiMMA; and Onera's Differential Inertial Vibrating Accelerometer (DIVA). Onera's DIVA design is of particular interest because it has an interesting mechanical isolating system that insulates the vibrating beam from the mounting base and protects the active part from thermal stresses due to the thermal expansion differences between quartz and the case material [Ref. 43]. In-run bias stability of $\sim 100 \mu\text{g}$ has been reported.

Two high-accuracy accelerometers are **MEMS resonant accelerometers**: Draper Laboratory's Silicon Oscillating Accelerometer (SOA) and Honeywell's Strategic Resonant Beam Accelerometer (SRBA). The SOA measures frequency change capacitively and has demonstrated performance of $1 \mu\text{g}$ and 1 ppm under independent laboratory testing [Ref. 44]. Figure 11(a) shows the Allan variance plots for two versions of the SOA. The velocity random walk for both versions is calculated (using the minus $\frac{1}{2}$ slope) to be $0.006 \text{ ft/s}/\sqrt{\text{h}}$. Figure 11(b) shows the small size (approximately 1 cu in) for a prototype instrument. The SRBA has piezoelectric frequency readout from high-purity single-crystal quartz material, coupled with well-established, robust oscillator circuit concepts [Ref. 45].

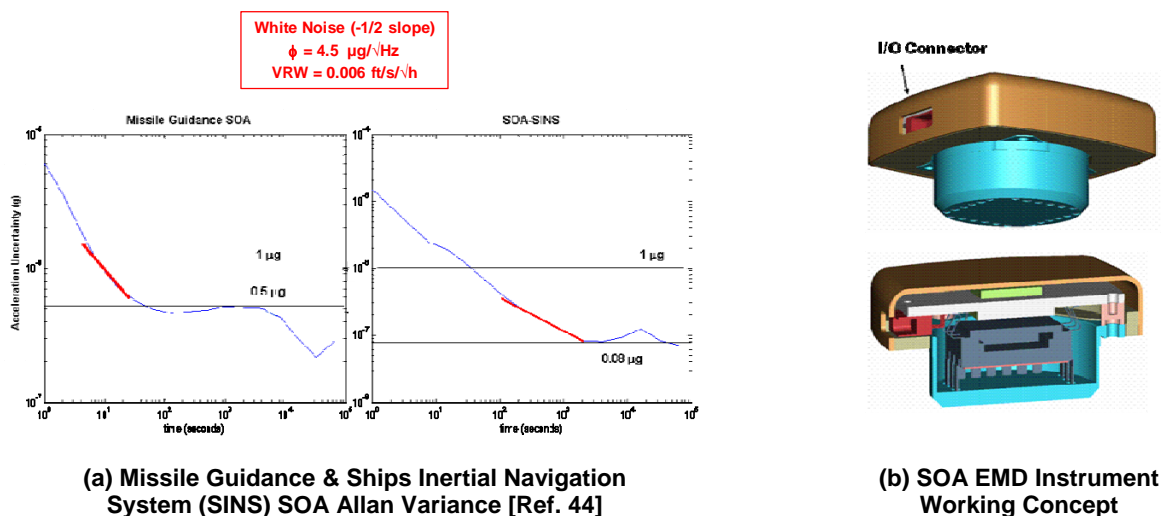
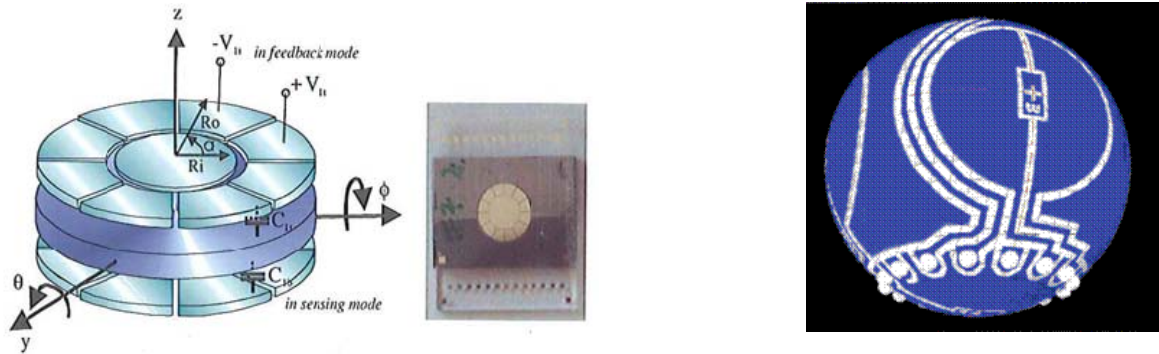


Figure 11: Silicon Oscillating Accelerometer (SOA).

2.4.1.3 Electrostatically-Levitated MEMS Accelerometers

Electrostatically levitating a proof mass eliminates the need to overcome the elastic restraint of mechanical supports. Theoretically, this would result in much higher sensitivity, less dependence on certain fabrication tolerances, and more flexibility in adjusting the device characteristics to bandwidth and sensitivity without the need to redesign flexures. A further advantage is the potential for multi-axis sensing from one device, i.e., they can operate as in-plane lateral displacement accelerometers and/or out-of-plane z-axis accelerometers. The major obstacle to development is the complexity of the control loop.

A levitated disk concept is under development at several organizations, including the University of Southampton (UK) and Berkeley Sensor and Actuator Center. Figure 12(a) [from Ref. 46] shows Southampton University's levitated disk concept in which the disk displacement is sensed capacitively and the loop closed with electrostatic forces. Another concept [Ref. 47] under development by Ball Semiconductor, Tokinec, Inc., Japan, and Tokohu University, Japan, is a levitated sphere. The 1-mm dia., 1.2-mg spherical proof mass with a deposited electrode pattern is shown in Fig 12(b). Position of the ball is sensed capacitively and closed-loop electrostatic forces maintain its position. During the MEMS fabrication process, the gap between the ball and outer shell is formed by a sacrificial layer of polysilicon, subsequently etched through the outer shell. For high-performance microgravity measurements in space, a noise floor of better than $40 \mu\text{g}/\sqrt{\text{Hz}}$ is expected.



(a) Levitated Disk – Electrode Configuration and Assembled 3-Layer Device [Ref. 46]

(b) Levitated 1 mm dia. Sphere with Electrode Pattern [Ref. 47]

Figure 12: Electrostatically-Levitated MEMS Accelerometers.

2.4.2 MEMS Gyroscopes

For inertial MEMS systems, attaining suitable gyro performance is more difficult to achieve than accelerometer performance. The Coriolis force is the basis for all vibratory gyroscopes. Basically, if a mass is vibrated sinusoidally in a plane, and that plane is rotated at some angular rate Ω , then the Coriolis force causes the mass to vibrate sinusoidally perpendicular to the frame with amplitude proportional to Ω . Measurement of the Coriolis-induced motion provides knowledge of Ω . This measurement is the underlying principle of all quartz and silicon micromachined **Coriolis Vibratory Gyros (CVGs)**. Fundamentally MEMS CVGs fall into three major areas: vibrating beams, vibrating plates, ring resonators. There are numerous MEMS CVGs available and under development worldwide [Refs. 34-37, 48]. As stated earlier, the performance of MEMS IMUs continues to be limited by gyro performance, which is currently around 5-30 deg/h in production.

2.4.2.1 MEMS Vibrating Beam (Tuning Fork) Gyros

In 1990, Systron Donner started initial production for the USAF Maverick missile, with 18,000 quartz rate gyros produced in 2 years. In the mid-1990s, the technology was applied to low-cost, high-volume production of yaw rate sensors, the first application being for Cadillac in 1997. Figure 13 shows Systron Donner's well-known H-shaped quartz gyro with piezoelectric drive and readout. These are in-plane gyros (i.e., they sense rate in the plane of the tuning fork). By 2008, over 40,000 rate gyros per day were being produced. High g versions have been developed for smart munitions. A 6-DOF IMU, containing three gyros and three vibrating accelerometers, the Digital Quartz IMU (DQI), was developed in 1992 and beyond. The DQI has been inserted in Rockwell's C-MIGITS [Ref. 49], to which Systron Donner has the production rights. Systron Donner is currently withdrawing from the automotive market to concentrate on higher performance sensors. A tactical-grade gyro with very low noise is being used in their all-quartz SDI500 tactical-grade IMU.

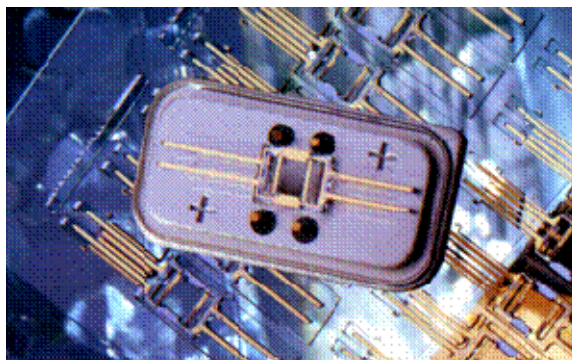


Figure 13: Systron Donner Quartz Rate Sensor (QRS)
 (© BEI Systron Donner Inertial Division, printed with permission).

Onera's Vibrating Integrated Gyro (VIG) has a specific insulating system for the vibrating elements (similar to their DIVA accelerometer) to reduce energy losses out of the structure. Output noise is $0.01 \text{ (deg/s)/}\sqrt{\text{Hz}}$ in a 100 Hz BW. Sagem's Quapason gyro has four quartz tines extending upward from a common base, thereby reducing unwanted cross-coupling from drive to sense [Ref. 50].

2.4.2.2 Vibrating Plate MEMS Gyros

Draper Laboratory's Tuning Fork Gyro-2 (TFG-2) shown in Figure 14 consists of two silicon proof mass plates suspended over a glass substrate by folded beams and vibrating in-plane 180 deg out of phase. This design is also referred to as a double-ended TFG. Dimensions are on the order of $300 \times 400 \mu\text{m}$. These are also in-plane gyros. The out-of-plane sense motion induced by the Coriolis force is detected by changes in capacitance between the proof mass and the substrates. For a typical MEMS gyro of this type, a 1-rad/s (in-plane) input rate results in a force of $\sim 9 \times 10^{-8} \text{ N}$ on the proof mass, $\sim 1 \times 10^{-9} \text{ m}$ of peak motion perpendicular to the sense electrodes, $\sim 3 \text{ aF}$ (10^{-18}) peak change in capacitance. Measuring 1 deg/h requires resolving motions of $\sim 5 \times 10^{-15} \text{ m}$ and about 0.25 electrons per cycle of motor motion. This technology has been transferred to Honeywell. Performance data indicate that the TFG currently performs at levels in the 3 to 50 deg/h range (3σ , compensated), over temperature ranges of -40°C to 85°C for many months and over shock inputs of up to 12,000 g. These have been evaluated in both the Extended Range Guided Munition Demonstration and the Competent Munitions Advanced Technology Demonstration (CMATD) Guided Artillery Shell [Ref. 51]. The Draper/Honeywell TFG series is a proven design for high-g applications and has undergone many iterations incorporating performance-enhancing features and fabrication improvements. The vibrating plate technology is used in Honeywell's HG1900, 1930, and 1940 IMUs; the latter being 2 cu in (33 cc).

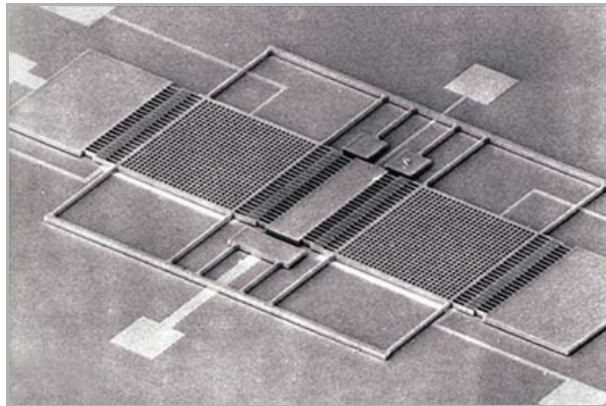


Figure 14: Top view of MEMS vibrating plate gyroscope (TFG-2).

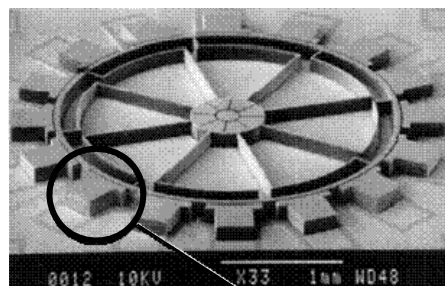
There are many kinds of vibrating plate gyros driven by the comb drive invented by the University of California, Berkeley. Many of the configurations have been designed to minimize coupling between sense and drive. Some are in-plane and some are z-axis gyros; some are oscillating circular disks. Studies indicate that the optimal gyro performance is achieved at a thickness of between 50 and 100 μm . Imperfections in the MEMS fabrication process can easily introduce unwanted performance errors, so continued evolution of advanced processes to build thicker, more 3-dimensional parts that are less susceptible to fabrication tolerances is critical to the performance and cost targets. Analog Devices now has a commercially available ADXRS gyro whose sense and drive axes are both parallel to the substrate, which allows operation in one atmosphere of gas, but at limited performance.

Other types of vibrating plate MEMS gyros that do not rely on the comb drive have been developed. These devices do not require such narrow gaps and tight fabrication tolerances as the comb drive. Jet Propulsion Lab's (JPL) MEMS gyro [Ref. 52], in which a 2-DOF resonating 4-leaf clover shape, suspended by four springs and containing a vertical post providing the main inertial mass, is driven in a rocking motion about an axis in the plane of the cloverleaf. This is an out-of-plane gyro (i.e., it responds to rate about the z-axis perpendicular to the plane of the clover leaf). A double gimbal structure driven and sensed electromagnetically has been developed in Japan [Ref. 53]. Sensoror Technologies (Norway) is developing the SAR500 novel, high-precision MEMS Butterfly gyro, designed to achieve an ARW of 0.002 $\text{deg}/\sqrt{\text{h}}$, in-run bias stability of 0.04 deg/h , and bias repeatability of 0.1 deg/h [Ref. 54]. The rate sensitive axis of the SAR500 lies in-plane with upper and lower sense plates that, aside from increasing sensitivity, allow for tuning of the sense and drive resonances and active compensation of the quadrature offset.

2.4.2.3 Resonant Ring MEMS Gyros

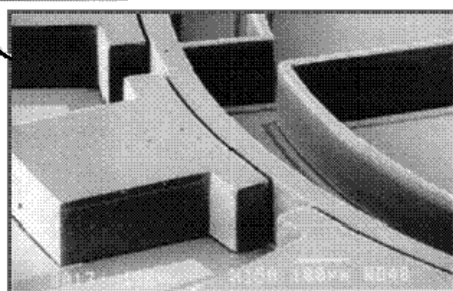
Resonant ring MEMS gyroscopes have an advantage in that the ring structure maintains the drive and sense vibrational energy all in one plane. However, there is also a disadvantage in that the ring has a low vibrating mass and hence lower scale factor. Figure 15(a) shows a single-crystal silicon vibrating ring gyro from U. Michigan [Ref. 55]. The ring vibrates at 20 kHz and is 2.7 mm diameter, 50 μm wide, and 150 μm high. The ring is electrostatically vibrated by the forcer electrodes into an in-plane, elliptically shaped, primary flexural mode. A rate about the z-axis (normal to the plane of the ring) excites the Coriolis force which causes energy to be transferred from the primary to the secondary flexural mode, 45 deg apart. The amplitude of the secondary mode is detected capacitively. Any frequency mismatches arising during fabrication can be electronically compensated by the balancing electrodes. Figure 15(b) shows the drive and sense flexural

modes before and after electronic balancing. This device has a scale factor of 132 mV/deg/s, resolution of 7.2 deg/h, and output noise of 10.4 deg/h/√Hz.

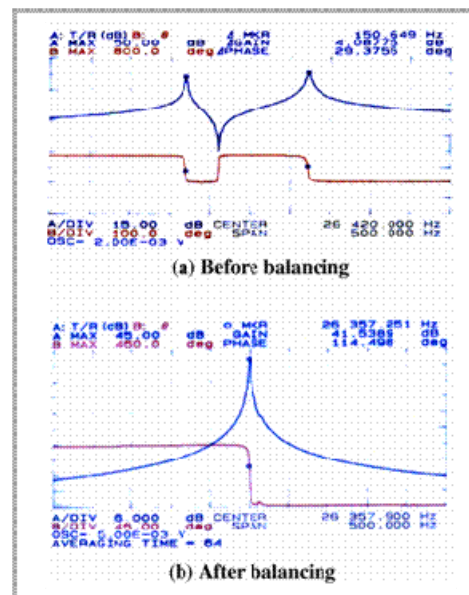


SEM picture of SCS vibrating ring gyroscope

Close-up view of ring structure, sense electrode, and 8-μm sense gap



(a) SEM Picture



(b) Effect of Balancing

Figure 15: U. Michigan Vibrating Ring Gyroscope [Ref. 55].

BAE Systems developed a Silicon Vibrating Structure Gyro (SiVSG) that consists of a ring resonator supported by compliant spokes. Coriolis-induced motion of the ring is detected by change in the magnetic field supplied by a central magnet. This inductive vibrating ring gyro [Ref. 56] was successfully used in an attitude reference system to control a production-standard, Medium-Range Tri-Nation Guided Anti-Tank (MR-TRIGAT) missile in flight in June 2000, as well as other military systems. An all-silicon capacitive vibrating ring gyro is under development. BAE's resonant ring technology now belongs to Atlantic Inertial Systems (AIS, part of B.F. Goodrich) and is incorporated in the SiIMU02 and SiNAV IMUs. AIS and Sumitomo Precision Products, Japan, have formed Silicon Sensing and are producing commercial-grade ring resonator gyro products in quantities of thousands per month, such as the DMU02 6-DOF dynamics measurement unit used in applications such as the Segway™ Human Transporter, or the CRS09 advertised as a general replacement for FOG gyroscopes in stabilization and GPS-aided navigation applications.

2.4.2.4 Non-Traditional MEMS Gyro Developments

There is strong indication that the traditional CVGs are unlikely to get much better than tactical-grade performance, so that other rate sensing technologies are being studied. One initiative is the DARPA Navigation Grade Integrated Micro Gyroscope (NGIMG) started in 2004 for navigation-grade MEMS gyros. The goal of the NGIMG program is to yield tiny (preferably chip-scale) gyros with performance around 0.001 deg/√h ARW, 0.01 deg/h bias uncertainty, <50 ppm scale factor, 300 Hz bandwidth, and <5 mW power [Ref. 57]. The early phase resulted in the selection of three MEMS technologies for further development (levitated spinning mass, micro- nuclear magnetic resonance (NMR), and quartz disk resonator).

Another DARPA initiative is the Microscale Rate Integrating Gyro (MRIG) study started in 2009. This is geared to overcoming another limitation of current MEMS gyros in that they only provide rate information directly and not angle. Although vibratory MRIGs are mentioned, this initiative specifically requires innovative approaches that will enable revolutionary advances in science, manufacturing, devices, or systems; specifically excluded are evolutionary improvements to the existing state of practice. Also, the European Space Agency (ESA) has funded several market analyses and feasibility studies based on European developments of MEMS gyros by companies such as BAE Systems (UK), Bosch (Germany), EADS CRC (Germany), LITEF (Germany), Sagem (France), SensoNor (Norway), and Thales (France). The desired goal is around 0.1 deg/h bias stability. In general though, it appears that production quantities of MEMS gyros with performance better than tactical grade is still many years away.

The difficulty in producing high performing small gyros created further interest in all-accelerometer systems (also known as gyro-free). Two approaches are typically used. In the first, the Coriolis effect is exploited and typically, three opposing pairs of monolithic MEMS accelerometers are dithered on a vibrating structure (or rotated). This approach allows the detection of angular rate. In the second approach, the accelerometers are placed in fixed locations and used to measure angular acceleration (also known as the 'direct' approach). In both approaches, the accelerometers also measure linear acceleration to provide the full navigation solution. However, in the direct approach, the need to make one more integration step makes it more vulnerable to bias variations and noise, so the output errors grow by an order of magnitude faster over time than a conventional IMU. To date, only systems of the first kind have been reduced to practice. One example is an IMU developed by L-3 Communications called the Micromachined Silicon Coriolis Inertial Rate and Acceleration Sensor (μ SCIRAS). Other examples are Kearfott's Micromachined Vibrating Beam Multisensor (MVBM) and Bosch's SMI540 multisensor.

2.4.3 Multi-Axis Gyro and Accelerometer Chips

Further size reductions have been achieved through the combination of two in-plane (x- and y-axis) and one out-of-plane (z-axis) sensors on one chip. Several vendors (e.g., InvenSense) have working devices with multiple sensors on a single chip, similar to those shown in Figure 16). Chips like these will result in IMUs around 0.2 cu in (3.3 cc). This is likely to be the ultimate in small IMUs enabling such things as personal navigation and guided bullets. It is likely that commercial investment will push this size-reduction technology, since there is a much stronger sized-based commercial need, rather than performance-based military need at this time. On-chip integration of other types of sensors (e.g., magnetometers) is another key element in further size and cost reduction. Current performance is suitable for commercial applications.

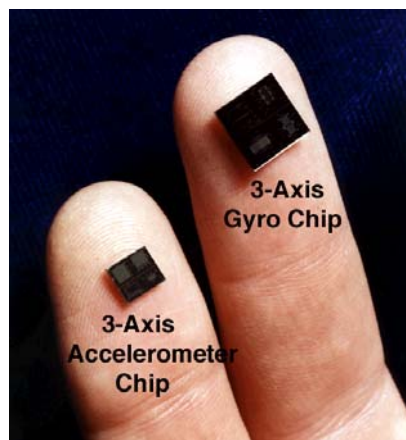
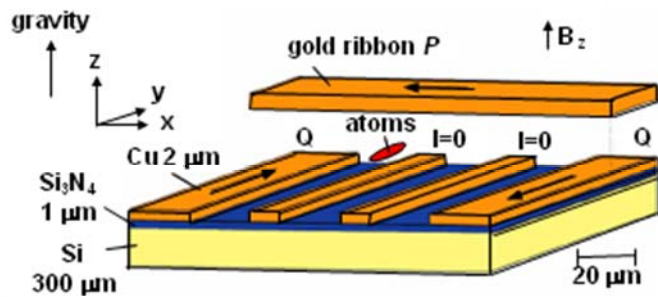


Figure 16: Photo of 3-Axis MEMS Chips.

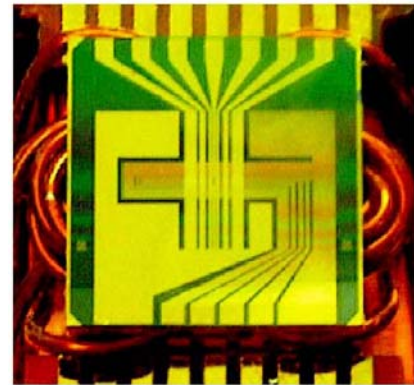
2.6 Cold Atom Sensors

A potentially promising technology, which is in its early development stages, is inertial sensing based upon atom interferometry (sometimes known as cold atom sensors), which exploits the wave nature of atoms. Since atoms have internal mass and structure, matter wave interferometry is analogous to light wave interferometry. In order to interfere a matter wave, an atom stream must be generated and then split, guided, and recombined. Laser cooling provides the required velocity control for the atom source. The cooling slows down the atoms so that (in comparison to the speed of a light wave) they will have more time (referred to as hang time) to experience the effects of angular rate or acceleration, and so have greater separation upon recombination. In theory, this means that atom interferometers could make the most accurate gyroscopes, accelerometers, gravity gradiometers, and precision clocks, by orders of magnitude [Refs. 58, 59]. There is much interest in atom interferometry and research is underway at many locations, such as Yale, Stanford, Massachusetts Institute of Technology, U. Arizona, AOSense Inc., Onera (France), and Draper Laboratory. A gravity gradiometer at Stanford University has demonstrated an accelerometer resolution of $10^{-11}g$ in 2007 using a differential accelerometer. Reference 60 presents the application of free fall atom interferometry for navigating future submarine platforms with real-time gravity error compensation.

Atom interferometer inertial sensors to date have used incoherent atoms propagating in free space, and laser pulse-based free space interferometers appear to offer the best potential for practical applications in the short to intermediate term. In the future, it may be possible to use coherent Bose-Einstein condensates for atom-guided interferometer structure, although problems of excitation of the internal degrees of freedom of the condensates, need for high vacuum, and the complex processes involved need to be overcome. Currently, atom interferometers and proof-of-concept atom interferometer gyros, accelerometers, and gradiometers are large, table-top sized experiments. However, miniaturization to a typical tactical-sized inertial sensor appears feasible. Reference 61 presents examples of using a microfabricated magneto-optic trap to coherently split and recombine Bose Einstein Condensates (BECs) in an interferometer. Figure 17 shows a schematic (a) and photo (b) of the MEMS fabricated magneto-optic trap. As fabricated, the MEMS magneto-optical trap chip size is 1.27 cm x 1.27 cm.



(a) Schematic of Magneto-optic Trap



(b) Microfabricated magneto-optic trap

Figure 17: Magneto-Optic Trap [Ref. 61].

If this technology can be developed, then it could result in a 5-m/h navigation system without GPS, in which the accelerometers are also measuring gravity gradients. The potential may ultimately exist for an all-accelerometer (including gradiometry) inertial navigation system. Miniaturization, while maintaining performance, is the most challenging aspect.

3.0 THE FUTURE

Inertial sensor technology maturity is depicted in Figure 18. Most of the technologies are in the lower-right hand corner, which represents a high maturity level. No new sensor technology appears to be on the near horizon, so what is next for the sensor designer? The desire for much lower cost and smaller size exists at all performance levels. Therefore, development over the next few years will continue to emphasize performance improvement and efficient packaging of MEMS sensors. Commercial applications require extremely low cost, so the payback will come from selling very large quantities (billions). Military applications desire low cost but the quantities are not so large (thousands to millions). The payback will be from providing the entire GN&C system, not just the sensors. This will be a worldwide effort with potential markets in the billions.

Inertial Navigation Sensors

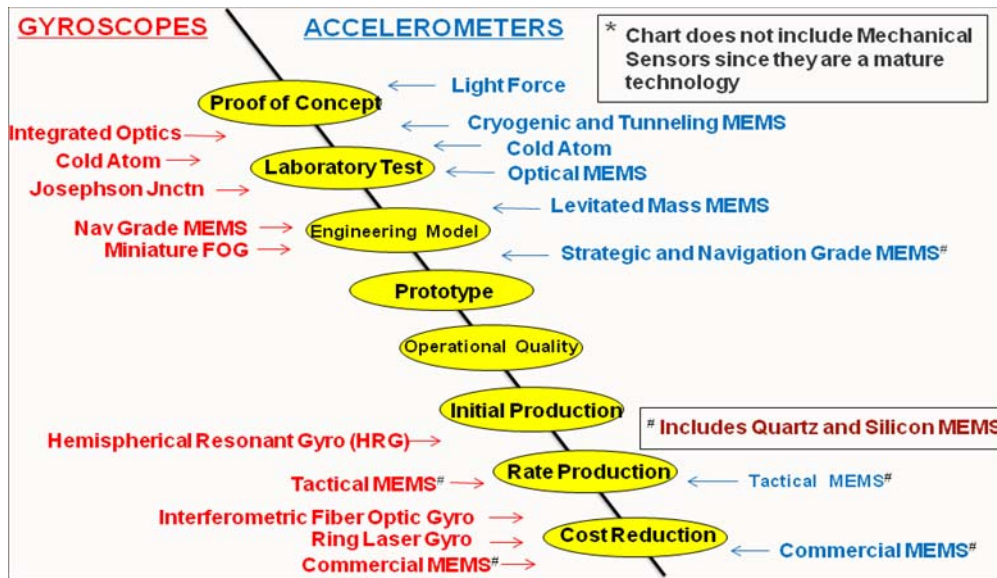


Figure 18: Inertial Sensor Technology Maturity.

Figure 19 shows an estimated timeline when the developing inertial technologies could meet their projected performance goals at the prototype level. Much of the monetary investment is still going into MEMS-type development activities, because of the enormous potential for MEMS to be used in numerous applications. Reference 62 estimates the MEMS inertial market to be \$3billion by 2013.

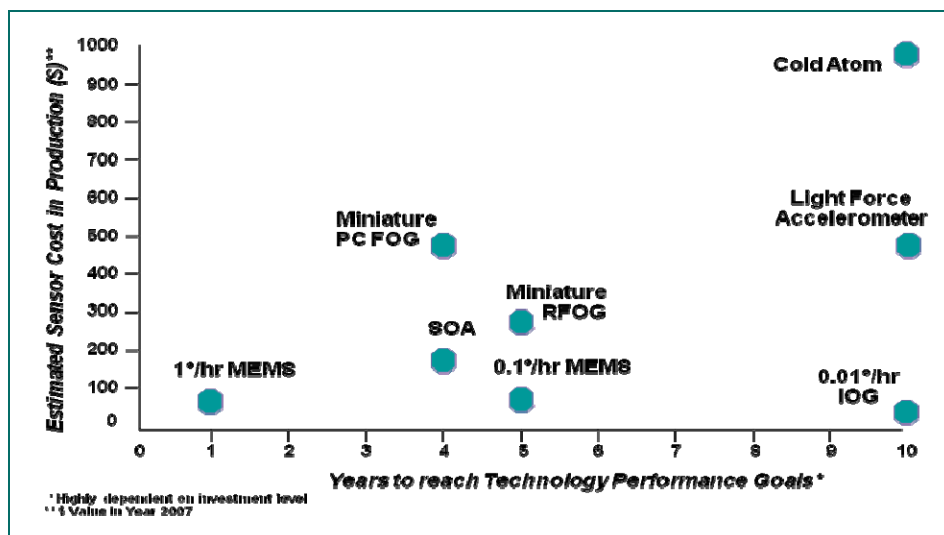


Figure 19: Inertial Technology Development Timeline to Prototype.

The potential market for navigation systems in GPS-unavailable environments is quite substantial as shown in Table 2. The cost and size goals are ultimate goals for the entire system, including inertial and augmentation sensors, and will be very difficult to achieve. Actual cost will depend on the number of units sold, so the cost

goals shown will only be attained in large quantities. However, it appears that this is a sufficiently lucrative market to provide payback for the expense of developing higher performance inertial sensors.

Table 2: Potential Market for Low-Cost Navigation Systems in GPS-Unavailable Environments.

Mission	Number of IMUs	Ultimate Cost Goal (k)	Ultimate Size Goal (cu in)
Personal/Soldier Navigation	100s of thousands	<1	<2
Distributed Networks	100s of thousands	<1	<2
Unmanned Land Vehicles	Thousands to tens of thousands	<5	<10
Unmanned Air Vehicles	Thousands	<10	<10
Unmanned Marine Vehicles	Thousands	<10	<10

In the immediate future, FOGs will continue pushing into areas traditionally held by RLGs. However, the continued development of a 2 cu in (33 cc) MEMS IMU with 1 deg/h performance will result in an IMU available for use in up to 80 percent of the tactical military applications. This will have a significant impact on the tactical RLG and tactical FOG market. The relatively large production number of these MEMS IMUs will result in some of the promised cost benefits from MEMS being realized. RLG and FOG systems will maintain a niche in areas where they have better performance than MEMS. FOGs may hold their ground if higher bend-radius fiber, such as photonic crystal fiber, results in smaller FOGs. Therefore, the development of miniature FOGs using photonic crystal fibers will continue, but only for applications at higher performance levels (e.g., navigation grade or better). The IOG is a true solid-state, optics-on-a-chip sensor, manufactured with MEMS-like batch processing, with the potential (theoretically) to provide navigation-grade performance or higher. This has the potential to be a winning technology, but requires significant monetary investment and technical advances to become feasible.

By overcoming such problems as limited dynamic range, long-term drift, high noise, turn-on repeatability, and initial transient response (especially for short time-of-flight and rapid reaction weapons such as guided bullets), the quest for MEMS performance improvement to tactical grade and beyond will continue to dominate inertial sensor technology investment. In 1998 [Ref. 34], it was pointed out that MEMS performance enhancement (noise) had improved by a factor of 10 every 2 years since 1991. While this has slowed in the last decade, MEMS inertial sensors still have the potential for over one order-of-magnitude performance improvement over the next decade by improved precision microfabrication, reduced sensitivity to packaging, and improved electronics. One technique for performance improvement that will likely continue is the attempt to gang multiple sensor arrays at the chip level together with the development of appropriate algorithms [Ref. 63]. This depends upon size reduction to be efficient, and on-chip packaging will be a key component. There will also be more strategic alliances between inertial developers/designers and MEMS/electronics suppliers similar to that between Thales (France) and Tronics Microsystems (France and U.S.) or Sensoror (Norway), PlanOptik AG (Germany), and Imego (Sweden). Also, the study of energy dissipation effects in MEMS resonators (such as thermoelastic damping, support losses, fluid losses, electrical damping, surface effects [Ref. 64]) will continue.

The rewards from the development of a MEMS gyro with navigation-grade quality (0.01 deg/h) would be enormous, so that initiatives like the DARPA NGIMG and MRIG will be observed closely. Effort will likely concentrate on rate sensing techniques that do not rely on Coriolis vibratory gyros. The concept of bypassing the gyro by developing a navigation grade **all-accelerometer** IMU requires accelerometers with accuracies on

the order of nano-g's or better and with large separation distances. Therefore, the use of all-accelerometer navigation for GPS-unavailable environments will not be viable until the far future, if ever.

Figure 20 shows possible future application areas for inertial sensor technology. Areas where FOGs are likely to remain unchallenged are in the fields of precision pointing and tracking and precision navigation (e.g., submarine). However, cold atom sensors are currently being developed as a very high performance, long-term competitor to FOG and mechanical systems, but it is still too early to predict with any confidence how this will turn out. In the very long term, we may possibly see Nano/Microengineered and Molecular Systems (NEMS) sensors and systems. One such development area is carbon nanotubes. Ultimately, navigation and position knowledge will soon become a commercial commodity item; everyone will expect to have it at all times. However, military navigation needs will continue to require higher-performance navigation sensors than commercially available, and it will be a difficult and expensive challenge to meet all requirements.

Very Precise Navigation	Long-Range Guidance	1 nm/hr Navigator	Tactical Weapons	Commercial Consumer
Accelerometer Technology				
Cold Atom	Cold Atom	MEMS	MEMS	MEMS
	MEMS			
Mechanical	Mechanical			NEMS
Gyro Technology				
Cold Atom	Cold Atom	IOG	MEMS	MEMS
	FOG	MEMS		
FOG	HRG			NEMS
	IOG	PCF FOG (MFOG)		

Figure 20: Future Applications for Inertial Sensor Technology.

ACKNOWLEDGMENTS

This paper is the latest updated version (for NATO SET-116 in 2011) of 'Inertial Navigation Sensors' that was previously presented at NATO Lecture Series SET-064 in 2003/2004 (Draper P-4151) and updated for SET-116 in 2008/2009 (Draper P-4701) and updated again for SET-116 in 2010 (Draper P-4994).

REFERENCES

- [1] Lawrence, A, *Modern Inertial Technology - Navigation, Guidance, and Control*, Springer-Verlag, Second Edition, 1998.
- [2] Barbour, N., "Inertial Components - Past, Present, and Future," Invited Paper, AIAA Guidance, Navigation, and Control Conference, Montreal, Canada, August 2001.
- [3] Mackenzie, D., *Inventing Accuracy - A Historical Sociology of Nuclear Missile Guidance*, MIT Press, 1990.

- [4] Britting, K., *Inertial Navigation Systems Analysis*, Wiley-Interscience, 1971.
- [5] Groves, P., *Principles of GNSS, Inertial, and Multisensor Integrated Navigation Systems*, Artech House, 2008.
- [6] Biezad, D., *Integrated Navigation and Guidance Systems*, AIAA Education Series, Editor-in-Chief J. Przemieniecki, AIAA, 1999.
- [7] Kuritsky, M. and M. Goldstein (Editors), *Inertial Navigation, Proceedings of the IEEE*, Vol. 71, No. 10, October 1983.
- [8] King, A., "Inertial Navigation - 40 years of Evolution," *GEC Review*, Vol. 13, No. 3, 1998.
- [9] Barbour, N. and W. Howell, *Inertial Navigation System*, McGraw-Hill Scientific Encyclopedia, (AccessScience @McGraw-Hill), 2006.
- [10] Jazwinski, A., *Stochastic Processes and Filtering Theory*, Academic Press, Inc., 1970.
- [11] IEEE Gyro and Accelerometer Panel, *IEEE Standard for Inertial Sensor Terminology*, IEEE Std 528-2001, 2001 (R2007).
- [12] IEEE Gyro and Accelerometer Panel, *IEEE Draft Standard for Inertial Systems Terminology*, P1559/D39, (R2008).
- [13] IEEE Gyro and Accelerometer Panel, *IEEE Draft Standard Specification Format Guide and Test Procedure for Inertial Measurement Units (IMU)*, P1780, (R2009).
- [14] IEEE Gyro and Accelerometer Panel, *IEEE Standard Specification Format Guide and Test Procedure for Linear, Single-Axis, Non-Gyroscopic Accelerometers*, IEEE Std 1293-1998, 1998 (R2008).
- [15] IEEE Gyro and Accelerometer Panel, *IEEE Standard Specification Format Guide and Test Procedure for Coriolis Vibratory Gyros*, 1431-2004, 2004.
- [16] IEEE Gyro and Accelerometer Panel, *IEEE Standard Specification Format Guide and Test Procedure for Single-Axis Interferometric Fiber Optic Gyros*, IEEE Std 952-1997, 1997 (R2008).
- [17] IEEE Gyro and Accelerometer Panel, *IEEE Standard Specification Format Guide and Test Procedure for Single-Axis Laser Gyros*, IEEE Standard 647-2006, April 2006.
- [18] IEEE Gyro and Accelerometer Panel, *IEEE Recommended Practice for Inertial Sensor Test Equipment, Instrumentation Data Acquisition, and Analysis*, IEEE Std 1554-2005, 2005.
- [19] Yahalom, R. et al., "Low-Cost, Compact Fiber-Optic Gyroscope for Super-Stable Line-of-Sight Stabilization," IEEE/ION PLANS, Indian Wells, CA, May 2010.
- [20] Hays, K. et al., "A Submarine Navigator for the 21st Century," IEEE PLANS, Palm Springs, CA, April 2002.

- [21] Sanders, S., L. Strandjord, and D. Mead, "Fiber-Optic Gyro Technology Trends - A Honeywell Perspective," Invited Paper, *2002 15th Optical Fiber Sensors Conference Technical Digest*, Vol. 1, pp. 5-82, August 2002.
- [22] Pavlath, G., "Fiber-Optic Gyros: The Vision Realized," 18th International Conference on Optical Fiber Sensors, Cancun, Mexico, October 2006.
- [23] Divakaruni, S. and S. Sanders, "Fiber Optic Gyros - A Compelling Choice for High Accuracy Applications," 18th International Conference on Optical Fiber Sensors, Cancun, Mexico, October 2006.
- [24] KVH Industries Inc., *An Update on KVH Fiber-Optic Gyros and Their Benefits Relative to Other Gyro Technologies*, March 2007.
- [25] Gaiffe, T., "From R&D Brassboards to Navigation Grade FOG-Based INS: The Experience of Photonics/Ixsea," Invited Paper, *2002 15th Optical Fiber Sensors Conference Technical Digest*, Vol. 1, pp. 1-4, August 2002.
- [26] Volk, C., J. Lincoln, and D. Tazartes, "Northrop Grumman's Family of Fiber-Optic Based Inertial Navigation Systems," IEEE PLANS 2006, San Diego, CA, April 2006.
- [27] Tawney, J. et al., "Photonic Crystal Fiber IFOGs," Optical Society of America, 18th International Conference on Optical Fiber Sensors, Cancun, Mexico, October 2006.
- [28] Sanders, G., L. Strandjord, and T. Qiu, "Hollow Core Fiber-Optic Ring Resonator for Rotation Sensing," 18th International Conference on Optical Fiber Sensors, Cancun, Mexico, October 2006.
- [29] Scheuer, J. and A. Yariv, "Sagnac Effect in Coupled Resonator Slow-Light Waveguide Structures," *Physical Review Letters*, Vol. 96, 053901, February 2006.
- [30] Steinberg, B. et al., "Slow-Light Waveguides with Mode Degeneracy: Rotation Induced Super Structures and Optical Gyroscopes," 18th International Conference on Optical Fiber Sensors, Cancun, Mexico, October 2006.
- [31] Wang, T. and S. Zhang, "(Study of the) Silicon Micromechanical Accelerometer Using an Optical Fiber," *Proc. SPIE, MEMS/MOEMS Technologies and Applications*, Vol. 4928, Conference, Shanghai, China, pp. 264-266, October 2002.
- [32] Morikawa, S., A. Ribeiro, R. Regazzi, L. Valente, and A Braga, "Triaxial Bragg Grating Accelerometer," *2002 15th Optical Fiber Sensors Conference Technical Digest*, Vol. 1, pp. 95-8, August 2002.
- [33] Waters, R., T. Jones, and J. Kim, "Micro-Electro-Mechanical-Systems (MEMS) Navigation Grade Electro-Optical Accelerometer (EOA)," NATO SET-104, Antalya, Turkey, September 2007.
- [34] Yazdi, N., F. Ayazi, and K. Najafi, "Micromachined Inertial Sensors," *Proc. of the IEEE*, Vol. 86, No. 8, August 1998.
- [35] El-Sheimy, N. and X. Niu, "The Promise of MEMS to the Navigation Community," *Inside GNSS*, March/April 2007.

- [36] DeAgostino, M. et al., "Performance Comparison of Different MEMS-Based IMUs," IEEE/ION PLANS, Indian Wells, CA, May 2010.
- [37] Allen, J., "Micro-System Inertial Sensing Technology Overview," *Sandia Report* SAND2009-3080, April 2009.
- [38] Weinberg, M. and A. Kourepenis, "Error Sources in In-Plane Silicon Tuning Fork Gyroscopes," *JMEMS*, Vol. 15, No. 3, 2006.
- [39] Stauffer, J-M. et al., "RS9000 a Novel MEMS Accelerometer Family for Mil/Aerospace and Safety Critical Applications," IEEE/ION PLANS, Indian Wells, CA, May 2010.
- [40] Dong, Y. et al., "High Performance Inertial Navigation Grade Sigma-Delta MEMS Accelerometer," IEEE PLANS, Indian Wells, CA, May 2010.
- [41] Liu, C. and T. Kenny, "A High-Precision, Wide-Bandwidth Micromachined Tunneling Accelerometer," *IEEE Journal of Microelectromechanical Systems* (ISSN 1057-7157), Vol. 10, No. 3, pp. 425-433, September 2001.
- [42] Dong, H. et al., "A Novel Out-of-Plane MEMS Tunneling Accelerometer with Excellent Low Frequency Resolution," 1st IEEE International Conference on Nano/Micro Engineered and Molecular Systems, Zhuhai, China, 2006.
- [43] Le Traon, O. et al., "The DIVA Accelerometer and VIG Gyro: Two Quartz Inertial MEMS for Guidance and Navigation Applications," IEEE/ION PLANS, Indian Wells, CA, May 2010.
- [44] Hopkins, R. et al., "The Silicon Oscillating Accelerometer: A High-Performance MEMS Accelerometer for Precision Navigation and Strategic Guidance Applications," ION 61st Annual Meeting, Cambridge, MA, June 2005.
- [45] Becka, S. et al., "A High Reliability Solid-State Accelerometer for Ballistic Missile Inertial Guidance," AIAA GN&C, Honolulu, HI, August 2008.
- [46] Houlihan, R. and M. Kraft, "Squeeze Film Effects in a MEMS Levitated Proof Mass," *Journal of Micromechanics and Microengineering*, Vol. 15, pp. 893-902, July 2005.
- [47] Toda, R. et al., "Electrostatically Levitated Spherical 3-Axis Accelerometer," MEMS 2002 - 15th IEEE International Conference on MEMS, Las Vegas, NV, January 2002.
- [48] Shkel, A., "Micromachined Gyroscopes: Challenges, Design Solutions, and Opportunities," *Smart Structures and Materials 2001, Proceedings of SPIE*, Vol. 4334, 2001.
- [49] Jaffe, R., T. Ashton, and A. Madni, "Advances in Ruggedized Quartz MEMS Inertial Measurement Units," IEEE/ION PLANS, Coronado, CA, April 2006.
- [50] Leger, P., "QUAPASON™ - A New Low-Cost Vibrating Gyroscope," 3rd St. Petersburg International Conference on Integrated Navigation Systems, St. Petersburg, Russia, May 1996.

- [51] Barbour, N. et al., “Evolution of Low-Cost MEMS Inertial Systems,” NATO SET Symposium on Emerging Military Capabilities Enabled by Advances in Navigation Sensors, Istanbul, Turkey, October 2002.
- [52] Bae, S., K. Hayworth, K. Yee, K. Shcheglov and D. Wiberg, “High Performance MEMS Micro-Gyroscope,” *Proc. SPIE, Design, Test, Integration, and Packaging of MEMS/MOEMS 2002*, Cannes, France, 2002.
- [53] Kasuzuke, M. et al., “Design, Fabrication and Operation of a MEMS Gimbal Gyroscope,” *Sensors and Actuators*, Vol. A121, May 2005.
- [54] Blixhavn, B. et al., “SAR500 - A Novel High Precision Gyroscope,” Symposium Gyro Technology, Stuttgart, September 2010.
- [55] He, G. and K. Najafi, “A Single-Crystal Silicon Vibrating Ring Gyroscope,” MEMS 2002 - 15th IEEE International Conference on Microelectromechanical Systems, Las Vegas, NV, January 2002.
- [56] Gripton, A., “The Application and Future Development of a MEMS SiVSG for Commercial and Military Inertial Products,” IEEE PLANS, Palm Springs, CA, April 2002.
- [57] <http://www.darpa.mil/mto/programs/ngimg>.
- [58] Gustavson, T., P. Bouyer, and M. Kasevich, “A Dual Atomic Beam Matter-Wave Gyroscope,” *SPIE*, Vol. 3270, pp. 62-68, 1998.
- [59] Kasevich, M. and C. Salomon - Editors, *Special Issue: “Quantum Mechanics for Space Application: From Quantum Optics to Atom Optics and General Relativity,” Applied Physics B*, Vol. 84, August 2006.
- [60] Rice H. and V. Benischek, “Submarine Navigation Applications of Atom Interferometry”, IEEE 2008 1-4244-1537-3
- [61] Zatezalo, A., “Bose Einstein Interferometry and its Application to Precision Undersea Navigation,” IEEE 2008, 1-4244-1537-3.
- [62] <http://www.yole.fr>, MEMS Accelerometer, Gyroscope and IMU Market 2008 – 2013, Yole Developpement, 2009.
- [63] Tanenhaus, M. et al., “Accurate Real Time Inertial Navigation Device by Application and Processing of Arrays of MEMS Inertial Sensors,” IEEE PLANS, Indian Wells, CA, May 2010.
- [64] Weinberg, M. et al., “Energy Loss in MEMS Resonators and the Impact on Inertial and RF Devices,” 16th International Conference on Solid State Sensors, Actuators, and Microsystems (Transducers 2009), Denver, CO, June 2009.